


## V<sub>4</sub> tetrahedral units in AV<sub>4</sub>X<sub>8</sub> lacunar spinels: Near degeneracy, charge fluctuations, and configurational mixing within a valence space of up to 21 *d* orbitals

L. Hozoi, M. S. Eldeeb, and U. K. Rößler

*Institute for Theoretical Solid State Physics, Leibniz IFW Dresden, Helmholtzstraße 20, 01069 Dresden, Germany*
 (Received 3 July 2019; accepted 2 April 2020; published 24 April 2020)

All properties of a given molecule or solid are determined by the way valence electrons are distributed over single-particle energy levels. For multiple, closely spaced single-particle levels, different occupation patterns may provide many-electron quantum states that are close in energy, interact, and admix. We address such near-degeneracy electron correlation effects for V<sub>4</sub> vanadium tetrahedral units as encountered in the lacunar spinel GaV<sub>4</sub>S<sub>8</sub>, explicitly taking into account up to 21 vanadium valence orbitals, and find effective orbital occupation numbers much different as compared to the picture previously laid out on the basis of mean-field calculations. In light of these results, a modified theoretical frame seems necessary to explain the peculiar magnetic properties of lacunar spinels and of related compounds.

DOI: [10.1103/PhysRevResearch.2.022017](https://doi.org/10.1103/PhysRevResearch.2.022017)

**Introduction.** Electrons within the *d* shells of transition-metal crystalline compounds are at the heart of an impressive variety of transport and magnetic properties that are not achievable in other, non-*d* valence-electron systems. Much of the exciting physics of *d*-shell materials relies on the presence of strong electron correlation effects, the transition-metal oxides and halides being typical examples. Since insulating phases are ubiquitous here, one approach in addressing these systems leans on a quasilocated representation of the *d* electrons, consideration of site symmetries via group theory, and real-space electronic-structure computations at various levels of sophistication (see, e.g., [1–4]); pioneered by Sugano *et al.* [1], it provides many-particle energy level diagrams that can explain the nature of the *d*-site ground-state (GS) configuration, the size of the GS spin moments, *d*-shell excitation spectra as measured, for example, by resonant inelastic x-ray scattering, etc. These energy level diagrams, also referred to as *d<sup>n</sup>* multiplet structure, turn out to be quite complex even when having two electrons only (or two holes [5]) within the single-ion five-orbital *d* shell. There are, however, systems for which the basic structural entity is an ionic fragment composed of more than one transition-metal site. With more *d* orbitals available within such a unit (dimer, trimer, etc.), the many-body *d*-level physics can become significantly more complicated. In particular, correlated multisite electronic states can emerge that span multiple molecularlike *d* orbitals [6–8]. This leads to properties that are remarkably different as compared to the case of single transition-metal centers.

As an eloquent illustration, we consider here the complex nature of the *d*-level electronic structure of clusters of vana-

dium ions in the lacunar-spinel compound GaV<sub>4</sub>S<sub>8</sub> [9]. Using quantum-chemical calculations based on extended multi-orbital spaces [10], we find near-degeneracy effects implying strong charge fluctuations across a group of a dozen molecularlike *d* levels. Since earlier quantum-chemical studies of *M*<sub>4</sub> metallic clusters such as tetrahedral Nb<sub>4</sub> [6] and of cubane-type ferredoxin proteins with a Fe<sub>4</sub>S<sub>4</sub> kernel [7,11] describe similar tight entanglement of several molecularlike electron configurations, it appears that this rich intracluster electronic structure with convoluted electron configurations spanning several sites is not restricted to GaV<sub>4</sub>S<sub>8</sub> and to the complex behavior encountered within the whole family of *AM*<sub>4</sub>X<sub>8</sub> lacunar spinels [9,12–14] but represents the behavior to be expected for electrons in small clusters of *d*-shell ions in general. The upshot is that the results of mean-field GS calculations relying on canonical density-functional theory (DFT) or extensions in the DFT + *U* category that incorporate Coulomb-repulsion terms [15] need to be taken with certain caution. This refers not only to the tendency of overestimating spin polarization in DFT computations [9,16–19] but also to more fundamental aspects, i.e., the very capability of providing a consistent physical picture when strong charge fluctuations within a whole manifold of electron configurations develop. In relation to the latter aspect, the noninteger occupancy of multiple one-electron levels becomes particularly important for the magnetic properties [7]. Finding here a many-body GS that is even qualitatively different from the GS presently proposed on the basis of DFT and DFT+*U* schemes implies that existing ideas and models for superexchange, effective magnetic interaction parameters, and magnetoelectric couplings [17] require reevaluation.

**Physical properties.** The family of *AM*<sub>4</sub>X<sub>8</sub> (or *A*<sub>1/2</sub>*M*<sub>2</sub>X<sub>4</sub>) chalcogenides has several members—the transition-metal ion can be V, Nb, Ta, Mo, or Re, *A* ∈ {Ga, Ge, Al}, and *X* ∈ {S, Se, Te}. Within this class of materials, GaV<sub>4</sub>S<sub>8</sub> stands out as the most fascinating compound. It undergoes a structural ferroelectric-ferroelastic transition at about 38 K, from a cubic

---

Published by the American Physical Society under the terms of the [Creative Commons Attribution 4.0 International](https://creativecommons.org/licenses/by/4.0/) license. Further distribution of this work must maintain attribution to the author(s) and the published article's title, journal citation, and DOI.

high-temperature phase (space group  $F-43m$ ) to a polar rhombohedral phase (space group  $R3m$ ), and then orders ferromagnetically at 16 K [9]. Owing to the polar low-temperature structure the magnetic phase diagram is very complex, with ferromagnetic, cycloidal, and field-induced skyrmion-lattice phases [12]. The coupling between skyrmions and electric polarization in the vicinity of such successive transitions may give rise to remarkable multiferroic properties, which hosts much potential for novel magnetoelectronic device concepts [13]. Indeed, a ferroelectric polarization of  $\sim 6000 \mu\text{C}/\text{m}^2$  has been measured [14] along the rhombohedral direction  $z \parallel [111]$ . Additionally, the value inferred for the spin-driven excess polarization,  $\sim 100 \mu\text{C}/\text{m}^2$  [14], is nearly two orders of magnitude larger than in  $\text{Cu}_2\text{OSeO}_3$  [20,21], a representative magnetoelectric material. Both the chiral spiraling magnetism and the magnetoelectric coupling derive from spin-orbit effects on the electronic structure and from cooperation between the coexisting electric and magnetic ordering modes. The remarkable instability of the cubic lattice structure is also intimately related to the underlying electronic structure of  $\text{V}_4$  tetrahedra, which is the focus of our investigation.

**Electronic structure, DFT-based picture.** The crystalline structure of the so-called lacunar (or deficient) spinels is related to the “perfect” spinels  $\text{AM}_2\text{X}_4$ . The important structural difference is that in a regular spinel each transition-metal site  $M$  is shared by two symmetry-equivalent  $M_4$  tetrahedra and has six symmetry-equivalent adjacent  $M$  ions (the same holds for the pyrochlore structure) while in the lacunar system  $\text{A}_{1/2}\text{M}_2\text{X}_4$  the A-site voids leave only three symmetry-equivalent  $M$  nearest-neighbor (NNs) [9]. In other words, the A-site voids (lacunae) imply  $M_4$  clustering, as for the “breathing”-pyrochlore lattice [22]. This structural feature, the insulating character, and the rich magnetic properties advocate the picture of  $M_4$ -tetrahedron quasilocated electrons and Mott physics, as discussed, for example, in Refs. [9,16,23]. Phenomenological analysis and DFT calculations point to a single-tetrahedron (see Fig. 1) molecular-orbital-like (MO) diagram with a set of  $a_1$ ,  $e$ , and  $t_2$  levels at the top of the valence orbital space (see, e.g., Refs. [9,16–19,23]), where the notations correspond to  $T_d$  point-group symmetry. Since DFT puts these  $t_2$  valence electronic levels at higher energy than the  $a_1$  and  $e$  components and having formally 1.75 electrons per transition-metal site ( $4 \times 1.75 = 7$  electrons per  $\text{V}_4$  tetrahedron, in  $\text{GaV}_4\text{S}_8$ ), the electronic structure of  $\text{GaV}_4\text{S}_8$  would then imply one unpaired electron ( $S = 1/2$ ) within the  $t_2$  sector ( $a_1^2 e^4 t_2^1$  GS electron configuration) [9,16–19,23]. However, given the findings of state-of-the-art quantum-chemical calculations on related systems having as a basic building block a tetrahedral  $d$ -metal unit— $\text{Nb}_4$  clusters [6] and ferredoxin complexes [7]—there are strong reasons to believe that this single-configuration picture presently put forward for the basic  $\text{V}_4$ -tetrahedron electronic structure in  $\text{AV}_4\text{X}_8$  lacunar spinels is too sketchy. We performed in this context embedded-cluster quantum-chemical computations and confronted results obtained on the basis of two different material models, as detailed in the following.

**Wave-function calculations,  $\text{V}_4$  tetrahedral unit.** In a first set of calculations, we adopted the simplest possible representation of the  $\text{GaV}_4\text{S}_8$  system: a  $\text{V}_4$   $d^7$  tetrahedral unit (in blue

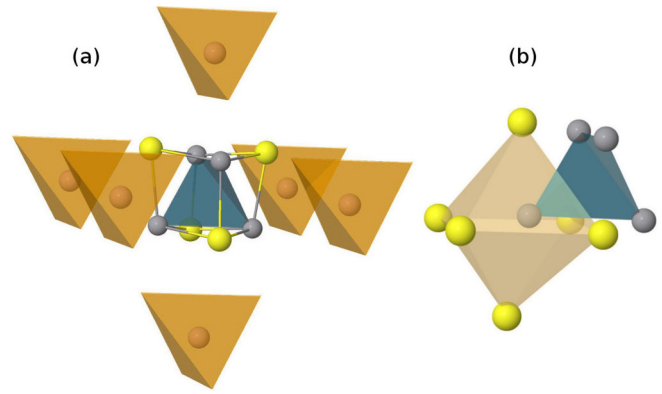


FIG. 1. (a)  $\text{V}_4$  tetrahedral unit (in blue) in  $\text{GaV}_4\text{S}_8$ , along with adjacent S sites (yellow spheres) and nearest-neighbor  $\text{GaS}_4$  tetrahedra (in dark orange, with S anions sitting at the vertices of the tetrahedra). The  $\text{V}_4$  and  $\text{GaS}_4$  tetrahedra are arranged as two interpenetrating fcc sublattices. The intratetrahedron V-V separation is  $2.90 \text{ \AA}$  while the distance between adjacent  $\text{V}_4$  tetrahedra is  $6.83 \text{ \AA}$  [9]. (b) The nearly octahedral S-ion cage around a V site is highlighted. There are two different V-S bond lengths:  $2.29$  and  $2.53 \text{ \AA}$  [9].

in Fig. 1) placed at the center of a large array of point charges, i.e., formal ionic point charges at the lattice positions within a given spatial domain plus a shell of additional charges at larger distances, the latter fitted to reproduce the Madelung potential in the central-tetrahedron region. The quantum-chemical package MOLPRO [24], effective core potentials plus valence-shell basis sets of triple- $\zeta$  quality [25,26] from the MOLPRO library, and high-temperature lattice parameters as reported for  $\text{GaV}_4\text{S}_8$  by Pocha *et al.* [9] were used. Having in mind the scenario of filled  $a_1$  and  $e$  levels and of a  $a_1^2 e^4 t_2^1$  GS configuration as derived by DFT investigations, we initially focused on active spaces comprising six V  $3d$  orbitals ( $a_1 + e + t_2$ -like) on top of the core ( $1s$  to  $2p$ ) and semicore ( $3s$ ,  $3p$ ) shells. Interestingly, severe convergence problems were encountered in those initial calculations (no convergence at all) but we were able to arrive to converged results when using four orbitals in the active space. The self-consistent-field (SCF) computations employing four active orbitals delivered a  $S = 1/2 a_1^2 t_2^5$  GS configuration. Since promoting an electron from  $a_1$  to  $t_2$  generates an electronic state described by a different irreducible representation, the four-orbital SCF calculation technically represents a single-configuration restricted open-shell Hartree-Fock (ROHF) computation [10].

To gain insight into correlation effects in this  $d$ -electron system, we next carried out a series of calculations in which the active orbital space is gradually enlarged to include more and more levels. This gradual augmentation of the active space was made after inspecting the sequence of virtual orbitals in the four-orbital SCF computation that provides the  $a_1^2 t_2^5$  GS. On top of the low-energy  $a$  and  $t$  MOs, we identified here a group of 17 other MOs with dominant V  $d$  character, of  $T$  ( $4 \times 3$ ),  $E$  ( $2 \times 2$ ), and  $A$  ( $1 \times 1$ ) symmetry; all those sum up to 21 MOs, which indicates that V  $4s$  and  $4p$  functions also contribute to some of the low-lying virtuals. Results of (full) configuration-interaction calculations based on active spaces

TABLE I. Relative energies, main configurations, and natural-orbital [10] occupation numbers for the lowest V<sub>4</sub>  $d^7$  CASCI roots when using active spaces of various dimensions (see text). The energy of the  ${}^2T$  ( $a^2t^5$ ) state obtained in the (four-orbital) ROHF calculation is taken as reference; electron occupation numbers are given per single orbital.

Number of active orbitals	Relative energies (eV)	Leading configuration(s)	Orbital occupation numbers				
			$a$	$t$	$e$	$t$	$t$
4	0	$a^2t^5$	2	1.67 ( $\times 3$ )			
6	-0.02	$a^2t^5$	2	1.67	0.00 ( $\times 2$ )		
9	-1.62	$a^2t^4e^1, a^2t^4t^1, \dots$	1.77	1.40	0.29	0.15	
12	-4.27	$a^2t^2e^3, a^2t^2e^1t^2, \dots$	1.29	0.91	0.56	0.43	0.19

comprising between 4 and 12 vanadium orbitals are provided in Table I. Such configuration-interaction computations are referred to in theoretical chemistry as complete-active-space configuration interaction (CASCI) [10]. Given the major difference between the DFT prediction for the single-tetrahedron GS configuration (i.e.,  $a^2e^4t^1$  orbital occupation) and the  $a^2t^5$  ROHF GS, a CASCI investigation represents the simplest way of finding hints to what are the crucial ingredients (e.g., the minimum number of vanadium orbitals to be considered in the reference active space) in order to achieve even a qualitatively correct description of the single-tetrahedron many-electron physics. Having this aspect clarified, remaining correlations—local residual fluctuations and connected fluctuations involving sites beyond one single V<sub>4</sub> tetrahedron—can in principle be accounted for through the computation of additional increments to the scattering operator  $|S\rangle$  used to express the correlated GS wave function [27].

Several aspects are striking in Table I. It is seen, first of all, that strong energy lowering effects occur when enlarging the active space to more than the lowest  $a$ ,  $t$ , and  $e$  levels (i.e., to more than six orbitals):  $\approx 1.6$  eV from 6 to 9 levels and  $\approx 2.6$  eV from 9 to 12; less dramatic modifications of the GS energy are reached only for active spaces comprising more than 12 orbitals (not shown in the table). Obviously, this has to do with dramatic modifications of the GS wave function once the active space becomes flexible enough, as illustrated in the third column of Table I. In the solid-state context, such effects were earlier discussed at the quantum-chemical level for the cobalt-oxide perovskite LaCoO<sub>3</sub> [28], although in LaCoO<sub>3</sub> the essential interactions refer to one single transition-metal ion and the corresponding ligand octahedron, i. e., single-site  $d-d$  plus ligand-to-metal charge-transfer-type correlations, and the relative energy shifts are less spectacular, in the range of 1 eV. Another example for relevant electron correlations on a  $MO_p$  unit is the recently discovered nickel-oxide superconductor Nd<sub>0.8</sub>Sr<sub>0.2</sub>NiO<sub>2</sub> [29], with  $p=4$  in the nickelate instead of  $p=6$  in LaCoO<sub>3</sub>. The present study draws attention to significantly more complex and therefore even more challenging physics occurring for *clustered*  $d$  ions (or clustered  $MX_p$  units) in solids.

Another important finding is that the  $a^2e^4t^1$  electron configuration, given as V<sub>4</sub>-tetrahedron GS configuration by periodic DFT calculations [9,16–19,23], is never one of the dominant configurations within the group of states representing the lower part of the spectrum. Further, even for the lowest-energy  $a$  orbital, the effective occupation number in the 12-orbital CASCI is much less than 2 ( $\approx 1.3$ , bottom line in

Table I). This is one other indicator for the extent of quantum charge fluctuations within the  $d$ -orbital manifold of the V<sub>4</sub> tetrahedron.

A  $t-e-t$  orbital sequence as indicated by the occupation numbers displayed in Table I was earlier reported for tetrahedral Nb<sub>4</sub> clusters [6]. A non-Aufbau filling (see the nature of the leading configurations for the larger active spaces in Table I) and strong configurational mixing were also stressed in Ref. [6]. Multiple low-lying configurations and strong  $d-d$  fluctuations were additionally pointed out by state-of-the-art quantum-chemical computations on closely related compounds such as the ferredoxin proteins [7,8]. Those are the most important findings in our investigation as well, i.e., complex genuine many-body physics involving more than half of the  $\sim 20$  single-tetrahedron one-electron  $d$  levels. Near degeneracy of multiple electron configurations and strong configuration-interaction effects as illustrated in Table I cannot be accounted for by mean-field constructions like DFT; such physics cannot be described either by post-DFT dynamical mean-field theory computations based on orbital spaces comprising only the lowest  $t$  or  $t+e$  levels (i.e., three [23] or five [16] orbitals).

*Wave-function calculations, [V<sub>4</sub>S<sub>16</sub>]embedded cluster.* To crosscheck the results obtained on the tetrahedral V<sub>4</sub> unit, more involved numerical investigations were performed on a significantly larger [V<sub>4</sub>S<sub>16</sub>] atomic cluster that includes the six NN sulfur anions around each transition-metal site. Four of these S neighbors form another tetrahedral entity, rotated with respect to the V<sub>4</sub> tetrahedron such that a distorted V<sub>4</sub>S<sub>4</sub> cube is realized (see Fig. 1). The other 12 S's are associated with vertices of the six GaS<sub>4</sub> tetrahedra drawn in dark-orange in Fig. 1(a). Although the latter anions feature somewhat longer S-V intersite distances [9], they form along with the former (four) distorted octahedral cages as depicted in Fig. 1(b). The embedding potential was generated for this [V<sub>4</sub>S<sub>16</sub>] fragment on the basis of a prior periodic Hartree-Fock calculation using the CRYSTAL program [30], following the type of methodology described in Refs. [28,31,32]. All-electron basis sets of triple- $\zeta$  and double- $\zeta$  quality were applied for vanadium [33] and sulfur [34], respectively.

Using insights from the smaller-cluster computations, we carried out complete active space self-consistent field (CASSCF) optimizations [10] for an active space of 12  $d$  orbitals. Also in this case, the resulting GS wave function has strong multiconfigurational character, with orbitals ordered in a  $a-t-e-t-a-e$  sequence as a function of increasing energies and dominant electron configurations of  $a^2t^2e^3$ ,  $a^2t^3e^2$ , and

$a^0t^4e^3$  type. The nature of the higher-energy orbitals in the active orbital space is found to be different in the two sets of calculations:  $t$  orbitals for the smaller  $[V_4]$  tetrahedral fragment (Table I) and  $a$  and  $e$  orbitals for the  $[V_4S_{16}]$  cluster. But all other features are consistent, although there are significant differences as concerns the computational details in the two sets of numerical investigations. CASSCF optimizations using 18 orbitals in the active space provide no qualitative modification of the GS wave function and occupation numbers of less than 0.05 for the additional orbitals in the active space (two sets of  $t$  orbitals).

**Conclusions.** In sum, the important aspect that our results bring to the fore is the rich single-tetrahedron many-body physics, with impressively strong configuration-interaction effects within a valence space of 12 or more orbitals. Near degeneracy and strong configurational mixing within a set of  $\sim 20$   $d$  orbitals are actually hardly surprising but nevertheless such effects were neglected so far in the study of the lacunar-spinel systems. One reason is the predominance of density-functional theory, essentially a mean-field theory, in computational materials science. Our CASCI and CASSCF results provide in this context strong motivation for more involved many-body *ab initio* investigations—CASSCF and post-CASSCF, using perhaps state-of-the-art density-matrix renormalization-group [7,35] or quantum Monte Carlo [35]

algorithms. Other related systems to be addressed by studies of this type are expected to reveal similarly complex electronic structures, also for different kinds of clusters of  $d$ -shell ions, including dimers and trimers. As for our example, a systematic analysis along the whole family of  $AM_4X_8$  lacunar spinels is required to better understand their peculiar magnetic properties. Most likely for heavier transition-metal species,  $4d$  and  $5d$ , second-order spin-orbit couplings will only increase the amount of multiconfigurational mixing. The fact that a  $M_4$  tetrahedron will generically display correlated superpositions of various electron configurations has important implications for the magnetism of the lacunar spinels. In particular, a rigid  $1/2$  spin as effective representation of the  $M_4$  tetrahedron and a  $S=1/2$  Heisenberg-Dzyaloshinskii-Moriya model for describing collective magnetism may then become inadequate. Non-Heisenberg features have remarkable consequences near the magnetic ordering temperature because the transversal spin-wave-like excitations and the longitudinal softness of magnetic moments are coupled via the chiral exchange and may stabilize precursor states composed of localized chiral spin fluctuations [36].

**Acknowledgments.** We thank A. Lubk, I. Kézsmárki, A. O. Mitrushchenkov, H. Stoll, V. Yushankhai, and P. Fulde for stimulating discussions and U. Nitzsche for technical assistance.

- 
- [1] S. Sugano, Y. Tanabe, and H. Kamimura, *Multiplets of Transition-Metal Ions in Crystals* (Elsevier, Amsterdam, 1970).
- [2] H. Ikeno, F. M. F. de Groot, E. Stavitski, and I. Tanaka, *J. Phys.: Condens. Matter* **21**, 104208 (2009).
- [3] M. W. Haverkort, M. Zwierzycki, and O. K. Andersen, *Phys. Rev. B* **85**, 165113 (2012).
- [4] L. Hozoi and P. Fulde, in *Computational Methods for Large Systems: Electronic Structure Approaches for Biotechnology and Nanotechnology*, edited by J. R. Reimers (Wiley, New York, 2011), Chap. 6.
- [5] For an analysis based on resonant inelastic x-ray scattering data and quantum-chemical embedded-cluster calculations of the  $Ni^{2+}$  two- $3d$ -hole configuration in  $La_2NiO_4$ , see the Supplemental Material in [37]. Many-body effects for the  $d^8$  configuration are also discussed in [29].
- [6] D. Majumdar and K. Balasubramanian, *J. Chem. Phys.* **121**, 4014 (2004).
- [7] S. Sharma, K. Sivalingam, F. Neese, and G. K.-L. Chan, *Nat. Chem.* **6**, 927 (2014).
- [8] D. Presti, S. J. Stoneburner, D. G. Truhlar, and L. Gagliardi, *J. Phys. Chem. C* **123**, 11899 (2019).
- [9] R. Pocha, D. Johrendt, and R. Pöttgen, *Chem. Mater.* **12**, 2882 (2000).
- [10] T. Helgaker, P. Jørgensen, and J. Olsen, *Molecular Electronic-Structure Theory* (Wiley, Chichester, 2000).
- [11] H. Beinert, R. H. Holm, and E. Münck, *Science* **277**, 653 (1997).
- [12] I. Kézsmárki, S. Bordács, P. Milde, E. Neuber, L. M. Eng, J. S. White, H. M. Rønnow, C. D. Dewhurst, M. Mochizuki, K. Yanai, H. Nakamura, D. Ehlers, V. Tsurkan, and A. Loidl, *Nat. Mater.* **14**, 1116 (2015).
- [13] M. Mochizuki, *Adv. Electron. Mater.* **2**, 1500180 (2016).
- [14] E. Ruff, S. Widmann, P. Lunkenheimer, V. Tsurkan, S. Bordács, I. Kézsmárki, and A. Loidl, *Sci. Adv.* **1**, e1500916 (2015).
- [15] B. Himmetoglu, A. Floris, S. de Gironcoli, and M. Cococcioni, *Int. J. Quantum Chem.* **114**, 14 (2014).
- [16] H.-S. Kim, K. Haule, and D. Vanderbilt, [arXiv:1810.09495](https://arxiv.org/abs/1810.09495).
- [17] S. A. Nikolaev and I. V. Solov'yev, *Phys. Rev. B* **99**, 100401(R) (2019).
- [18] H. Lee, M. Y. Jeong, J.-H. Sim, H. Yoon, S. Ryee, and M. J. Han, *Europhys. Lett.* **125**, 47005 (2019).
- [19] Y. Wang, D. Puggioni, and J. M. Rondinelli, *Phys. Rev. B* **100**, 115149 (2019).
- [20] S. Seki, X. Z. Yu, S. Ishiwata, and Y. Tokura, *Science* **336**, 198 (2012).
- [21] M. Belesi, I. Rousochatzakis, M. Abid, U. K. Röbber, H. Berger, and J.-P. Ansermet, *Phys. Rev. B* **85**, 224413 (2012).
- [22] Y. Okamoto, G. J. Nilsen, J. P. Attfield, and Z. Hiroi, *Phys. Rev. Lett.* **110**, 097203 (2013).
- [23] A. Camjayi, C. Acha, R. Weht, M. G. Rodríguez, B. Corraze, E. Janod, L. Cario, and M. J. Rozenberg, *Phys. Rev. Lett.* **113**, 086404 (2014).
- [24] H. J. Werner, P. J. Knowles, G. Knizia, F. R. Manby, and M. Schütz, *WIREs: Comput. Mol. Sci.* **2**, 242 (2012).
- [25] M. Dolg, U. Wedig, H. Stoll, and H. Preuss, *J. Chem. Phys.* **86**, 866 (1987).
- [26] J. M. L. Martin and A. Sundermann, *J. Chem. Phys.* **114**, 3408 (2001).
- [27] P. Fulde, *J. Chem. Phys.* **150**, 030901 (2019).
- [28] L. Hozoi, U. Birkenheuer, H. Stoll, and P. Fulde, *New J. Phys.* **11**, 023023 (2009).
- [29] M. Jiang, M. Berciu, and G. A. Sawatzky, [arXiv:1909.02557](https://arxiv.org/abs/1909.02557).
- [30] R. Dovesi, R. Orlando, B. Civalieri, C. Roetti, V. R. Saunders, and C. M. Zicovich-Wilson, *Z. Kristallogr.* **220**, 571 (2005).

- [31] L. Hozoi, U. Birkenheuer, P. Fulde, A. Mitrushchenkov, and H. Stoll, *Phys. Rev. B* **76**, 085109 (2007).
- [32] V. M. Katukuri, K. Roszeitis, V. Yushankhai, A. Mitrushchenkov, H. Stoll, M. van Veenendaal, P. Fulde, J. van den Brink, and L. Hozoi, *Inorg. Chem.* **53**, 4833 (2014).
- [33] M. F. Peintinger, D. V. Oliveira, and T. Bredow, *J. Comput. Chem.* **34**, 451 (2013).
- [34] A. Schäfer, H. Horn, and R. Ahlrichs, *J. Chem. Phys.* **97**, 2571 (1992).
- [35] N. A. Bogdanov, G. L. Manni, S. Sharma, O. Gunnarsson, and A. Alavi, [arXiv:1803.07026](https://arxiv.org/abs/1803.07026).
- [36] H. Wilhelm, M. Baenitz, M. Schmidt, U. K. Rößler, A. A. Leonov, and A. N. Bogdanov, *Phys. Rev. Lett.* **107**, 127203 (2011).
- [37] G. Fabbris, D. Meyers, L. Xu, V. M. Katukuri, L. Hozoi, X. Liu, Z.-Y. Chen, J. Okamoto, T. Schmitt, A. Uldry, B. Delley, G. D. Gu, D. Prabhakaran, A. T. Boothroyd, J. van den Brink, D. J. Huang, and M. P. M. Dean, *Phys. Rev. Lett.* **118**, 156402 (2017).